The Assembly History of the Galactic Stellar Halo Traced by Carbon-Enhanced Metal-Poor Stars

Young Sun Lee[1], Timothy C. Beers[2], and Young Kwang Kim[1]

[1]*Department of Astronomy and Space Science, Chungnam National University, Daejeon 34134, South Korea*

[2]*Department of Physics and JINA-CEE, University of Notre Dame, Notre Dame, IN 46556, USA*

Abstract

We present an analysis of the kinematic properties of Galactic halo stars, using over 100,000 main sequence turnoff (MSTO) stars observed in Sloan Digital Sky Survey (SDSS). After separating the MSTO stars into an inner-halo region (IHR) and outer-halo region (OHR), based on the spatial variation of their [C/Fe], we find that stars in the OHR show a clear retrograde motion of -49 km/s and a more spherical distribution, while stars in the IHR exhibit zero net rotation (-3 km/s) with a much more radially biased distribution. Moreover, after classifying carbon-enhanced metal-poor (CEMP) stars among the MSTO sample into CEMP-s and CEMP-no objects by their absolute carbon abundances, we examine the spatial distributions of the fractions of CEMP-no and CEMP-s stars and the kinematics of each sub-class. The CEMP-no stars are the majority sub-class of CEMP stars in the OHR (~65%), and the minority sub-class in the IHR (~44%). The CEMP-no stars in each halo region exhibit slightly higher counter-rotation and a more spherical distribution of orbits than the CEMP-s stars. These distinct characteristics provide strong evidence that numerous low-mass satellite galaxies have donated stars to the OHR, while more-massive dwarf galaxies provided the dominant contribution to the IHR.

Main Sequence Turnoff Stars

Our sample consists of main-sequence turnoff (MSTO) stars observed during the course of the SDSS (York et al. 2000). One big advantage of this sample is that they do not suffer from dilution of the carbon material due to extra mixing occurring for giants. Stellar parameters ($T_{\rm eff}$, log g, and [Fe/H]), [C/Fe], and distance of each star are derived from the SEGUE Stellar Parameter Pipeline (Lee et al. 2011, 2013). The final sample was selected by the following criteria: 12 ≤ S/N, 15.5 ≤ g_0 ≤ 19.2, 0.22 ≤ $(g-r)_0$ ≤ 0.38, 3.5 ≤ log g ≤ 4.8, and 5600 K ≤ $T_{\rm eff}$ ≤ 6700 K. We used proper motions from Gaia Data Release 2 (Gaia collaboration et al. 2018) to calculate the velocity components of our sample.

Construction of Carbonicity Map

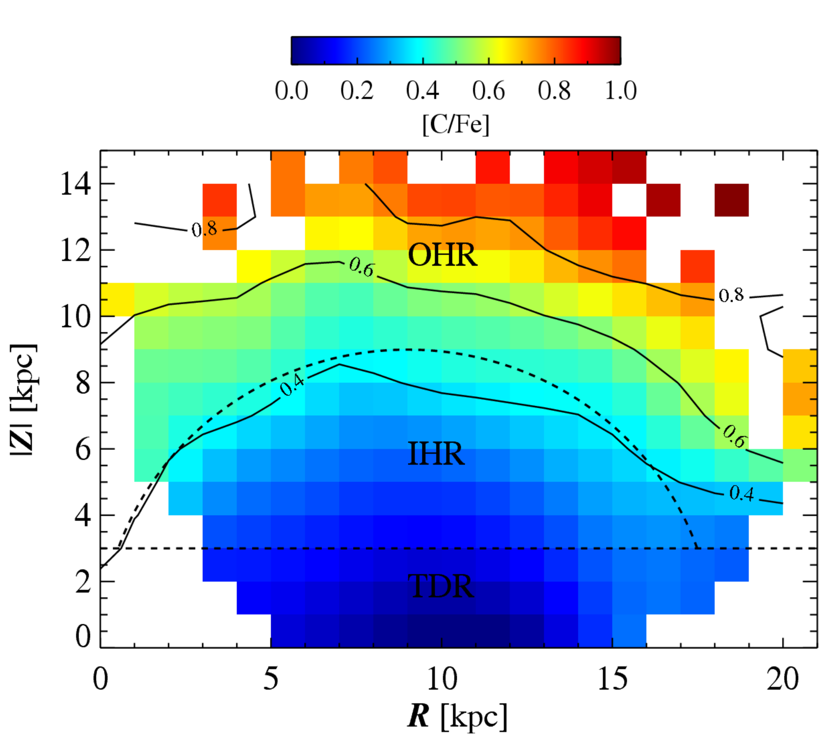

- Using the measure [C/Fe], we first constructed a carbonicity map.
- It clearly shows an enhanced level of [C/Fe] with increasing |Z|, implying that the varying level of [C/Fe] may be associated with different stellar populations.
- Based on the contrasts, we separate into tree regions: thick-disk region (TDR), inner-halo region (IHR), and outer-halo region (OHR).

Velocity Dispersions of the Galactic Halo

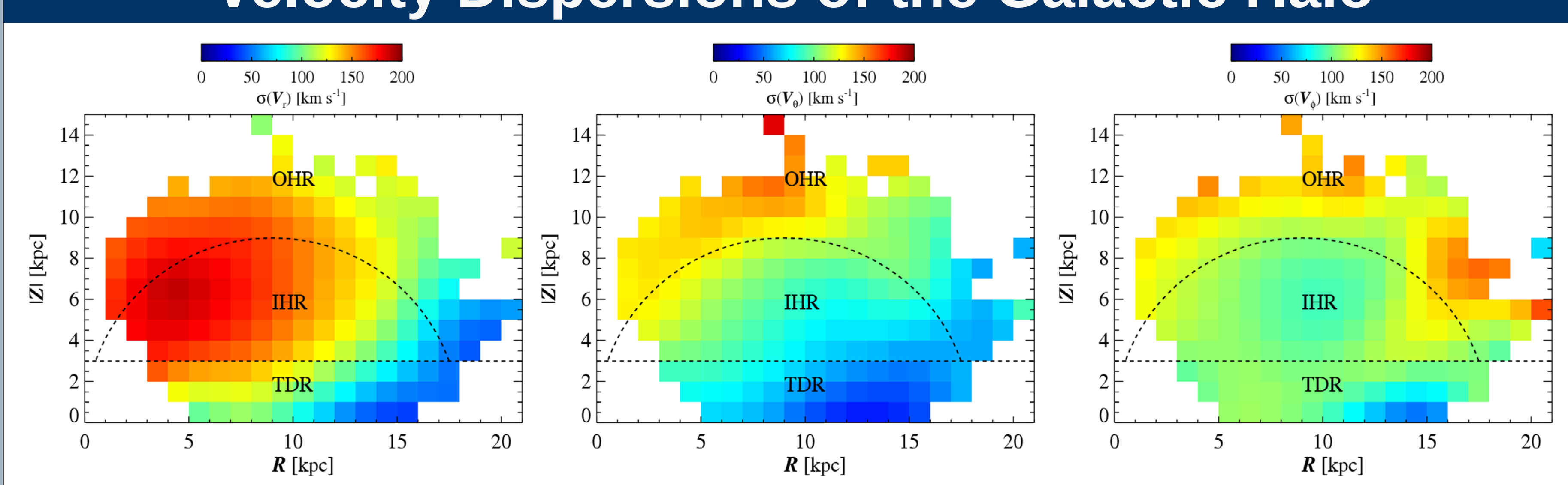

The maps of the dispersions of V_r, V_θ, and V_φ components in the |Z| and R plane reveal the following:

- The dispersion becomes higher towards the bulge and Galactic north pole. At a given |Z|, it shows a clear radial gradient, while the V_θ dispersion exhibits a moderate vertical gradient. However, there exists no strong dispersion gradient in V_φ within the IHR, although the dispersion increases in the OHR.
- The population with high radial dispersion in the direction toward the Galactic center supports the identification by numerous recent studies of the *Gaia Sausage* (Belokurov et al. 2018) or *Gaia-Enceladus* (Helmi et al. 2018).
- The boundary (dashed curve) defined in the carbonicity map between the IHR and OHR corresponds well with differences in the V_θ and V_φ dispersions, which suggests that the chemical division of the stellar populations can identify distinct kinematic properties as well.

Separation of CEMP-s and CEMP-no Stars

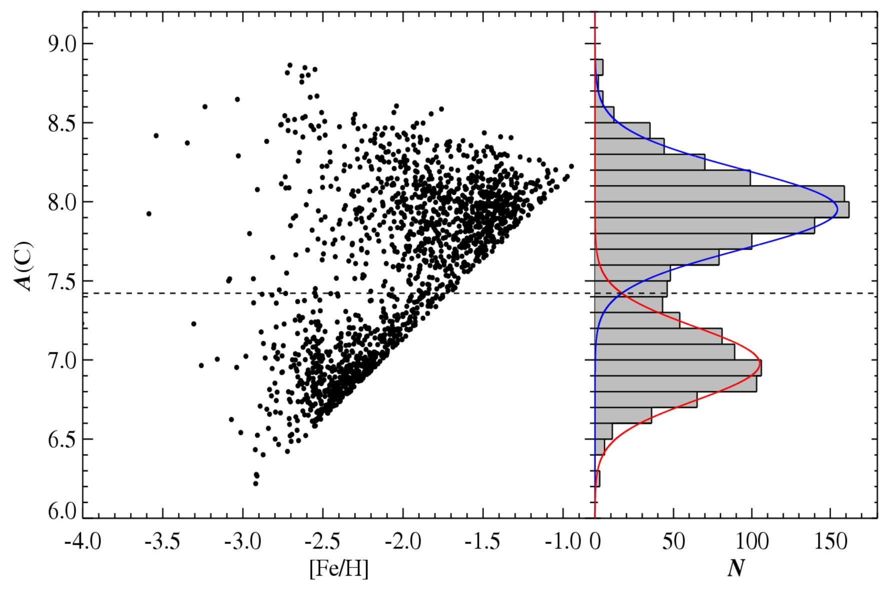

- We followed Yoon et al. (2016) to separate CEMP stars into CEMP-s and CEMP-no objects using the absolute carbon abundance, A(C).
- We consider as CEMP-no stars below the gray-dashed line in the [Fe/H] – A(C) diagram.

Fraction of CEMP-no Stars Among CEMP Stars

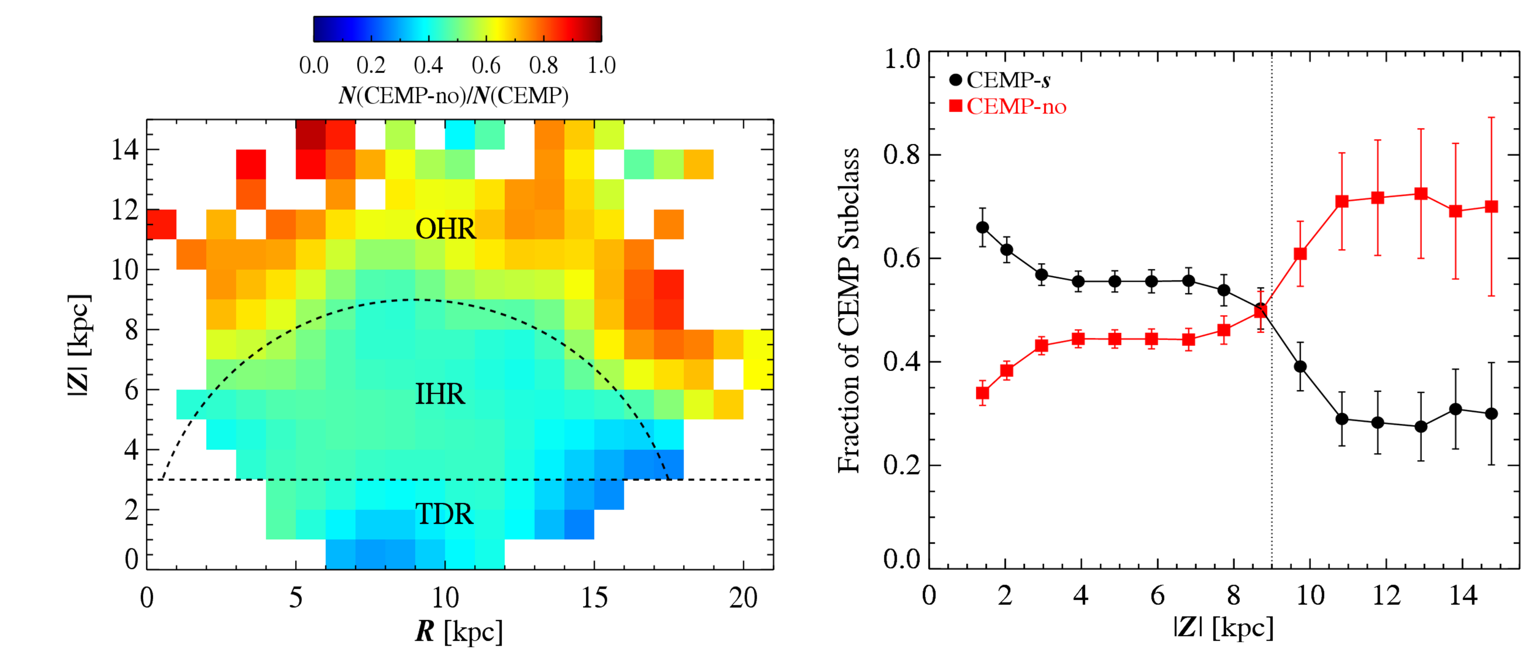

- The map and profile of fractions of CEMP-s and CEMP-no stars clearly show the increasing fraction of CEMP-no stars with increasing |Z|, and the occurrence of a transition region at |Z| ~ 9 kpc from the CEMP-s to CEMP-no dominated, which agrees with the dividing distance between the IHR and OHR.
- As progenitor masses of the CEMP-s and CEMP-no objects differ, the different fractions of CEMP-s and CEMP-no stars between the IHR and OHR suggest the different origins of the two halo populations, likely involving different progenitor masses.

Summary of Kinematic Properties of CEMP Stars

Region	Subclass	V_r (km s^{-1})	V_θ (km s^{-1})	V_φ (km s^{-1})	σ_{V_r} (km s^{-1})	σ_{V_θ} (km s^{-1})	σ_{V_φ} (km s^{-1})	β
TDR	CEMP-s	3±4	-2±2	15±3	143±3	81±3	104±2	0.58±0.02
	CEMP-no	-1±5	-7±4	1±4	132±4	101±3	102±3	0.41±0.04
IHR	CEMP-s	-1±3	-6±2	-18±2	153±2	100±2	103±2	0.56±0.02
	CEMP-no	-1±4	-4±3	-26±3	141±2	120±3	116±2	0.30±0.03
OHR	CEMP-s	-8±10	-18±10	-46±9	158±7	145±10	120±7	0.29±0.10
	CEMP-no	-2±10	-22±11	-60±9	137±6	139±8	133±7	0.01±0.11

- Among CEMP stars, both CEMP-s and CEM-no stars show significant retrograde motion in the OHR, while moderate counter-rotating signature in the IHR. Generally, the CEMP-no stars show more retrograde signal.
- The anisotropy parameter β is consistently lower for the CEMP-no stars than that for the CEMP-s within a given halo component. Considering all stars in the IHR and OHR, the derived β for the IHR is 0.63 and 0.28 for the OHR.
- These imply that the CEMP-no stars exhibit a more isotropic velocity ellipsoid than the CEMP-s stars, and the stellar orbits in the OHR have a more isotropic distribution, but a more radial-biased distribution in the IHR.

Implications on the Formation of the Galactic Halo

- Since the progenitor mass (> 20 $M_\odot$) range of CEMP-no stars differs from that (< 4 – 5 $M_\odot$) of CEMP-s stars, the larger fraction of CEMP-no stars in the OHR implies that the dominant progenitors of the current inner- halo and outer-halo stars differ.
- The larger retrograding signal and lower anisotropy parameter in the OHR kinematically support the above claim, as the CEMP-no stars in the OHR have more chance of being accreted from numerous low-mass satellites.
- From these results, we can conclude that the two halos have undergone different assembly histories; the outer halo mostly consists of stars from disrupted satellites such as ultra faint dwarf galaxies around the Milky Way**.**

References

Belokurov, V., et al. 2018, NMRAS, 478, 611
Gaia Collaboration, et al. 2018, A&A, 616, 1
Helmi, A., et al. 2018, Nature, 563, 85
Lee, Y. S., et al. 2008, AJ, 136, 2022
Lee, Y. S., et al. 2013, AJ, 146, 132
Yoon, J., et al. 2016, ApJ, 833,20
York, D. G., et al. 2000, AJ, 120, 1579